Available online at www.sciencedirect.com
SCIENCE DIRECT®
Journal of Nuclear Materials 335 (2004) 379–386
journal of nuclear materials
www.elsevier.com/locate/jnucmat

Long-lived activation products in TRIGA Mark II research reactor concrete shield: calculation and experiment

Tomaž Žagar [a,*], Matjaž Božič [b], Matjaž Ravnik [a]

[a] *Reactor Physics Department, Jožef Stefan Institute, Jamova 39, 1000 Ljubljana, Slovenia*
[b] *Nuklearna elektrarna Krško, Vrbina 12, 8270 Krško, Slovenia*

Received 20 October 2003; accepted 27 July 2004

Abstract

In this paper, a process of long-lived activity determination in research reactor concrete shielding is presented. The described process is a combination of experiment and calculations. Samples of original heavy reactor concrete containing mineral barite were irradiated inside the reactor shielding to measure its long-lived induced radioactivity. The most active long-lived (γ emitting) radioactive nuclides in the concrete were found to be ^{133}Ba, ^{60}Co and ^{152}Eu. Neutron flux, activation rates and concrete activity were calculated for actual shield geometry for different irradiation and cooling times using TORT and ORIGEN codes. Experimental results of flux and activity measurements showed good agreement with the results of calculations. Volume of activated concrete waste after reactor decommissioning was estimated for particular case of Jožef Stefan Institute TRIGA reactor. It was observed that the clearance levels of some important long-lived isotopes typical for barite concrete (e.g. ^{133}Ba, ^{41}Ca) are not included in the IAEA and EU basic safety standards.

PACS: 28.50.Dr; 28.41.Qb; 28.41.Te

1. Introduction

Interest for studies of residual radioactivity in concrete shields is increasing as more and more research and power reactors approach decommissioning and dismantling. Until recently, there were practically no published experimental data on activation of concrete shields in research reactors. This is particularly true for special concrete types containing heavy minerals (e.g. barite $BaSO_4$) which are frequently used as shields for research reactors. In addition the activation analyses of the neutron shields are not interesting only for research reactors decommissioning planning, but also for shielding new reactor concepts such as accelerator driven multiplying systems or in fusion reactors.

A method for determination of concrete activation based on combination of experimental activation analysis of the concrete samples and detailed calculations of the activation distribution in the shield of TRIGA Mark II research reactor is presented in this paper. Due to the heterogeneity and geometrical complexity of the reactor shield, the calculations are the only non-destructive method for predicting the activation of all its parts. The experimental determination of the reactor shield

* Corresponding author.
E-mail address: tomaz.zagar@ijs.si (T. Žagar).

0022-3115/$ - see front matter © 2004 Elsevier B.V. All rights reserved.
doi:10.1016/j.jnucmat.2004.07.047

activation is used in complement to the calculations. The need for supporting the calculations with experiment is based on the fact, that long-lived activity in concrete is mainly due to trace-elements (e.g. cobalt, europium,...) [1]. They are natural constituents of basic concrete materials and their concentrations can vary from case to case.

The geometry of TRIGA research reactor at J. Stefan Institute (JSI) in Ljubljana, Slovenia is schematically presented in Fig. 1. It is typical for all TRIGA Mark II reactors built by General Atomics. The reactor power is 250 kW. The core is placed at the bottom of the 2-m-diameter open tank filled with water (detailed description of the core can be found in [2]). The water tank is surrounded by biological shielding made of barite concrete (heavy concrete). Dimensions of the reactor structures are presented in Figs. 1 and 2. In radial direction reactor geometry roughly consist of cylindrical core, annular graphite reflector, annular region of water, cylindrical aluminium reactor tank and thick radiological shield made of barite concrete. The geometry of the shield in axial direction is practically uniform. The irregularities in the geometry are mainly due to horizontal experimental channels in form of aluminium tubes of ≈20-cm diameter passing through the radiological shield and ending near or at the reactor core.

Experiments for verification of activation calculations inside the biological shield were performed in one of the radial experimental channels, denoted as irradiation channel number 4 in Fig. 1. The experimental environment in the bulk concrete was reproduced as accurately as possible, since the calculation analysis showed that even small deviations from the actual irradiation environment significantly change the neutron spectrum and the total flux. To reproduce the environment of the bulk concrete shielding a special sample-holder, aluminium tube filled with cylindrical concrete inserts, was designed to fit in irradiation channel number 4. Horizontal irradiation channel number 4 is a radial tube that extends from the reflector assembly through the water and concrete to the outer face of the shield structure. The sample-holder (Fig. 2) is filled with removable concrete inserts, which have prefabricated holes for inserting samples, which are 1.2 cm in diameter and 2.0 cm in length. All together there are eight sample holes, evenly distributed along the sample-holder. During the irradiation, when the sample-holder is inserted in the channel, the first sample hole is at the position of the inner surface of the reactor shield, that is 98.4 cm from the reactor core centre in radial direction. The other sample positions are at depths of 5, 10, 20, 30, 40, 50 and 60 cm from the concrete inner surface, as presented on vertical cross-section through sample-holder in Fig. 2.

2. Description of the calculation model

The calculation of the activation rate of selected nuclides anywhere in the biological shielding or in the irradiation channel is performed in two steps. In the first step the neutron flux spatial and energy distribution in the entire reactor body is calculated in multi-group transport approximation. In the second step, the activation of selected nuclides is calculated. The main problem

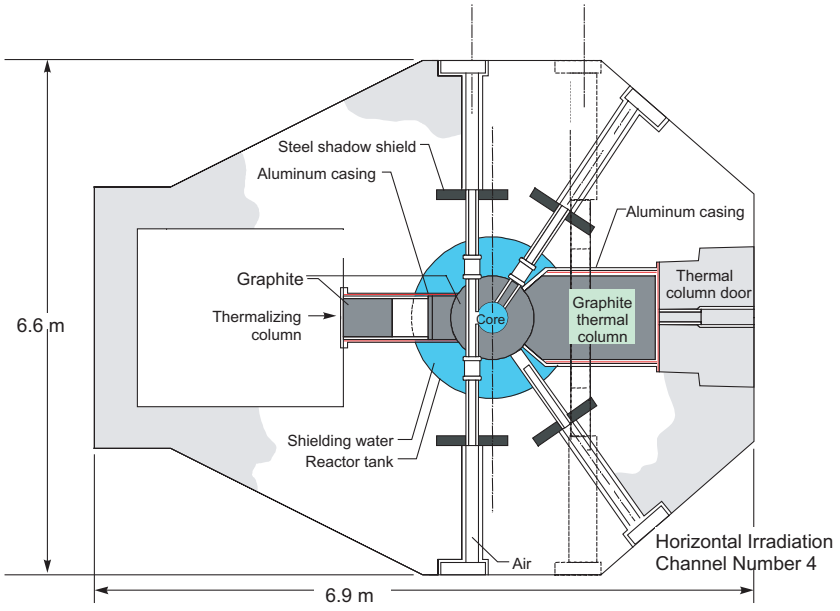

Fig. 1. Horizontal cross-section through TRIGA Mark II research reactor at core mid-plane.

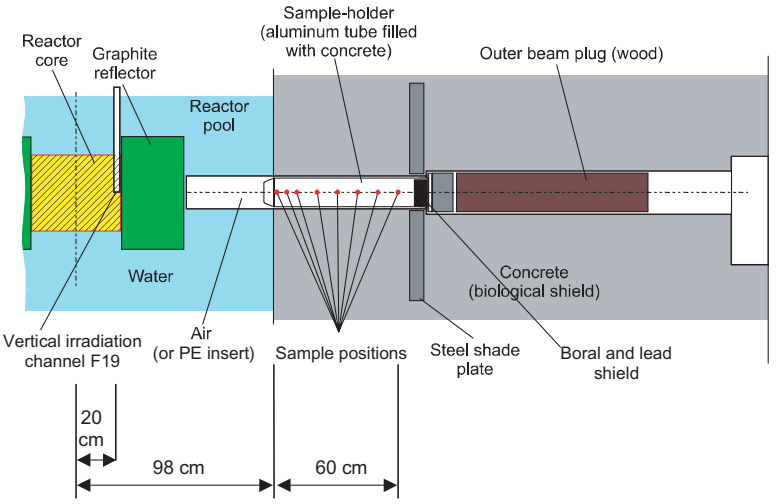

Fig. 2. Vertical cross-section through TRIGA Mark II research reactor in direction of horizontal irradiation channel number 4. The irradiation channel number 4 is filled with sample-holder used for irradiation of samples and plugged with wooden plug. The air region in front of sample-holder is either empty (filled with air) or filled with polyethylene (PE) insert.

in the first step is developing the physical model of the reactor that is at least as accurate as the measurements and at the same time practically feasible due to computing limitations. In the second step effective multi-group neutron capture cross-sections for the nuclides typical for the concrete are needed. Several precursors of the long-lived activation products (e.g. ^{59}Co, ^{132}Ba, ^{151}Eu,...) are found in the concrete. They are not typical reactor nuclides and for this reason they are not usually included in the libraries routinely used with the transport codes. The activation rates for nuclides present in used transport library (e.g. ^{198}Au) were directly calculated together with the flux distribution. The activation of other nuclides was calculated using the calculated flux as input in a dedicated computer code for isotopic generation and depletion (ORIGEN-S [3]).

The flux distribution in the reactor core, in the tank and in the biological shield was calculated in 47-group three-dimensional neutron transport approximation. Deterministic S_N transport code TORT [4] was used with 47 neutron group cross-section library BUGLE-96 [5]. Detailed reactor geometry was considered in r–φ–z geometry. The reactor body (the bulk radiological shield), water tank and graphite reflector were reproduced in the calculation model in all details, in particular taking into account irradiation channels and other cavities, while the reactor core was treated as a homogeneous region. Composition of the materials used was reproduced to the best of our knowledge. Detailed analysis of computational model optimisation and verification is presented in separate report [6], where also detailed description of used material and geometry data can be found. Only final results of these computational analyses are repeated here for completeness.

In the final model, the calculations were performed using 177 600 mesh points and S_{10} approximation. Typical running time on Pentium 3 computer is about 15 h. The discretization error of the model was estimated to be less than 0.001 in total neutron flux and approximately 0.01 in the group flux. Uncertainties in material data were also assessed, especially concrete density and hydrogen content were subjected to additional analysis. Parametric study of hydrogen concentration [6] showed that 1% increase in concrete density or 2% increase in water concentration in concrete increased the thermal flux gradient trough the sample-holder for 3% (relative increase in all cases).

The calculated total flux was normalised to experimental value measured in the vertical irradiation channel at core mid-plane (denoted F19 in Fig. 2). The irradiation channel F19 is located at the core boundary situated 20 cm from the reactor core centre. The experimental value of total neutron flux in this channel at the core mid-height and at nominal operating power 250 kW is 6.54×10^{12} (1 ± 0.03) cm^{-2} s^{-1} [7]. The normalised calculated flux distribution along the axis of the experimental channel is presented in Fig. 3 for three cases. In the first, the part of the channel near the core is assumed to be empty (filled with air), in the second case, this part is assumed to be filled with polyethylene insert. Both cases were also realised during experimental irradiation. In the third, hypothetical case, the whole section of this channel in the reactor pool between concrete shielding and graphite reflector is replaced with water. It can be observed that the flux drops for two orders of magnitude, if the cavity in front of the sample-holder is filled with water. The effect does not disappear with increasing radial distance as could be expected due to relatively

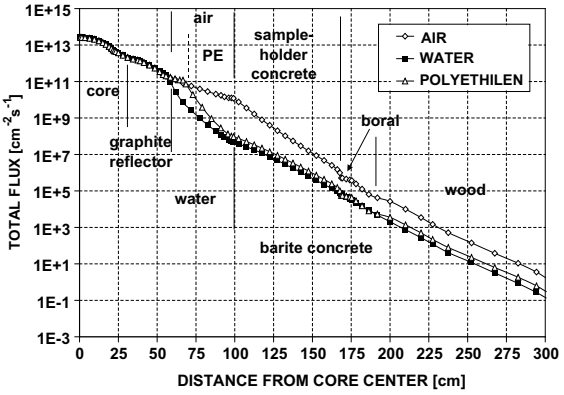

Fig. 3. The normalised calculated flux distribution along the radial axis of the experimental channel 4 used for samples irradiation. The part of the channel close to the core is modelled with three different materials: air (upper curve), polyethylene (middle curve), and filled with water (lower curve).

small transverse dimensions of the perturbation. This can be explained by the fact that mainly uncollided neutrons contribute to the flux deep in the target. Even small volume of strong fast neutron scatterer (water) throws long and sharp neutron 'shadow' far into the shield material. The analogue is true also for the empty regions or regions filled with material with low scattering cross-section for fast neutrons, e.g. aluminium. Neglecting such details in the calculation model may result in unacceptably high error in the calculated flux and consequently, activation rate distribution.

3. Description of the experiment

In order to validate the calculations, the calculated activation rates were compared to the experimental results measured in the irradiation channel in the reactor shield. Two sets of experiments were performed using the sample-holder in the channel 4. In the first experiment, the flux was measured using two standard neutron activation detectors (nickel and gold foils). The purpose of this experiment was to evaluate the calculated flux distributions. In the second experiment, the samples taken from concrete reactor shield were irradiated. The purpose of this experiment was to confirm and evaluate the calculated activation rates for the most important nuclides.

3.1. Flux measurement and comparison to flux calculations

Gold foils used for the flux measurements were in the form of pure gold thin discs (8 mm in diameter and 50 μm thick) and 0.1% diluted gold wires (1 mm in diameter). Nickel wires were made of 99.982% pure nickel in form of thin wires (0.75 mm in diameter). For cadmium ratio determination diluted gold wires were irradiated inside cadmium tubes with 0.5 mm thick walls. All foils were irradiated for approximately one day at full reactor power without interruptions. Measured reaction rates for $^{197}Au(n,\gamma)^{198}Au$, $^{64}Ni(n,\gamma)^{65}Ni$ and $^{58}Ni(n,p)^{58}Co$ reactions in gold and nickel foils in eight different concrete depths and for two different irradiation conditions (with and without polyethylene insert) are presented in Table 1. Calculated and measured values of the ^{198}Au reaction rates under the same irradiation conditions are compared in Fig. 4.

The calculated neutron flux used for ^{198}Au reaction rate calculation was normalised to measured value in the irradiation channel F19, relatively far away from the concrete shielding. Nevertheless, the calculated slope of ^{198}Au reaction rates in concrete approximately 1 m from core centre presented in Fig. 4 shows excellent agreement with the measured results. The relative experimental error was estimated to be in the order of 0.1 and can be attributed mainly to the inaccuracy of reactor power calibration and gamma spectroscopy method used for measuring activity. The discrepancy between the measured and calculated activities may be explained by uncertainties in material composition (mainly concrete density and hydrogen content as already mentioned in description of calculations method), simplified geometry in the model (planar surfaces approximated by cylindrical finite differences) and by rough neutron group structure applied in the calculations. Due to small number of thermal groups and neglected up-scattering in the BUGLE-96 library [5], the thermal reaction rates are underestimated in the calculations. However the improvement of the calculation model can be achieved only by using more detailed cross-section library.

Measured cadmium ratio in sample-holder without polyethylene insert for reaction rates on ^{198}Au in four different concrete depths are presented in Table 2. From these results the shift towards harder spectrum with increasing depth is evident.

3.2. Concrete activation measurement

The concrete samples were taken from barite concrete blocks made of the same materials and the same time as the reactor body of TRIGA reactor at JSI. Sample chemical composition is presented in Table 3. The values presented in the first column of this table were taken from design reports on experimental concrete composition found in reactor archives. Results of experimental analyses performed recently using the chemical analytical methods [8], neutron activation analysis (NAA) [9] and the X-ray fluorescence analysis (XRFA) [10] are presented in second column. We can see that

Table 1
Measured saturated activity per one parent atom for gold and nickel foils irradiated in sample-holder with and without polyethylene insert between core and biological shielding surface

Concrete depth (cm)	Without polyethylene insert (air only)			With polyethylene insert	
	^{198}Au (Bq)	^{65}Ni (Bq)	^{58}Co (Bq)	^{198}Au (Bq)	^{58}Co (Bq)
0 (surface)	4.5×10^{-12} (1 ± 0.07)	5.8×10^{-14}	1.4×10^{-16}	7.3×10^{-14} (1 ± 0.05)	4.4×10^{-18}
5	1.8×10^{-12} (1 ± 0.06)	2.4×10^{-14}	7.9×10^{-17}	5.0×10^{-14} (1 ± 0.06)	3.2×10^{-18}
10	8.6×10^{-13} (1 ± 0.06)	1.3×10^{-14}	4.6×10^{-17}	3.0×10^{-14} (1 ± 0.09)	2.2×10^{-18}
20	1.7×10^{-13} (1 ± 0.05)			8.8×10^{-15} (1 ± 0.03)	
30	3.9×10^{-14} (1 ± 0.05)			2.9×10^{-15} (1 ± 0.03)	
40	1.1×10^{-14} (1 ± 0.05)			1.1×10^{-15} (1 ± 0.03)	
50	3.1×10^{-15} (1 ± 0.05)			4.2×10^{-16} (1 ± 0.03)	
60	9.2×10^{-16} (1 ± 0.05)			1.5×10^{-16} (1 ± 0.03)	

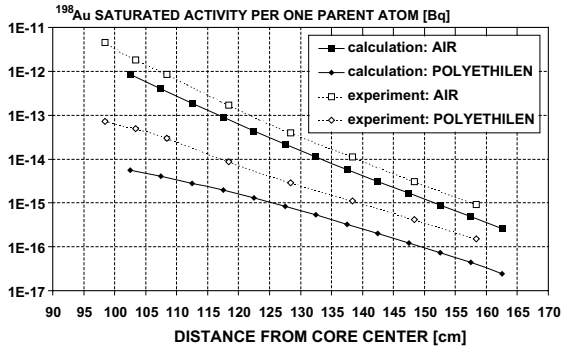

Fig. 4. Measured (dotted curves) and calculated (solid curves) saturated activity per one parent atom for gold irradiated in different depths of the sample-holder. The upper two curves correspond to irradiation layout without polyethylene insert (air only), the lower two curves correspond to irradiation of samples behind PE insert.

Table 2
Measured cadmium ratio (R_{Cd}) on diluted gold wires in sample-holder without polyethylene insert

Concrete depth (cm)	$R_{Cd}=\frac{\phi\sigma_{act}(total)}{\phi\sigma_{act}(Cd\ covered)}$ {^{198}Au(n, γ)}
0 (surface)	5.14 (1 ± 0.14)
5	5.27 (1 ± 0.13)
10	5.05 (1 ± 0.13)
20	4.34 (1 ± 0.12)

Table 3
Composition of barite concrete samples

Element	Design data (wt%)	Experimental data (wt%)
Ba	48.1	44.3 (±3.0)
O	32.4	
S	11.4	7.5 (±2.0)
Ca	4.2	6.7 (±2.0)
Si	1.0	1.4 (±0.5)
Mg	0.7	1.9 (±0.5)
C	0.6	
Fe	0.6	0.68 (±0.05)
H	0.6	
Al	0.4	
Co		3.92E−04 (±1.6E−05)
Cs		1.23E−04 (±6E−06)
Eu		1.7E−05 (±2E−06)
Sm		7.6E−05 (±8E−06)
Th		1.18E−04 (±6E−06)
U		1.2E−04 (±4E−05)
Zn		0.017 (±0.0008)

experimental results agree with the design data. The design data (presented in the first column of Table 3) was assumed to be good representation of the average concrete composition in our reactor and as such used as input data for flux and activation calculations. Data on trace element concentrations for gamma emitting isotope production (Co, Cs, Eu and Zn) were taken from the second column of Table 3. Direct chemical measurement of hydrogen in this concrete samples was not performed, since hydrogen loss in this concrete is expected to be very small. This is due to two factors: First, gamma heating of concrete is very small in this low power research reactor. Second, the whole concrete shield was covered with special bitumen coating at the time of reactor construction to prevent hydrogen loss from concrete. This additional note on hydrogen concentration in concrete, which has strong influence on flux distributions in reactor shield, was added in proof.

Concrete samples were homogenised and filled into small cylindrical vials for irradiation. Outer dimensions of the vial were 1.0 cm in diameter and 1.2 cm in height. Concrete samples were irradiated for 100 h at full reactor power in order to achieve sufficient activation of long-lived activation products for gamma spectroscopy measurements. The 100 h irradiation time was accumulated in several intervals of 20–30 h uninterrupted irradiation, due to practical limitation on reactor operation. The error due to interruptions in irradiation is calculated to be smaller than 3% for long-lived nuclides with half-lives about one year long. This contribution to experimental error is evaluated for each nuclide separately (Ref. [11]

or [12]) and is accounted for in reported experimental results.

Before concrete sample activity measurements were performed, the samples were cooled from four to eight months to improve the accuracy of measured long-lived nuclides activities. The gamma activity of the irradiated concrete samples was measured using a Princeton Gamma-Tech (PGT) HPGe detector type NIGC 26 with a FWHM resolution of 2.00 keV at 1.33 MeV, connected to a multi-channel pulse-height analyzer based on The Nucleus Personal Computer Analyzer (PCA-II) card. The minimum detectable gamma ray energy of our detector configuration was 30 keV. Natural gamma-ray background of the detector was checked, and no special gamma peaks were found. Radioisotopes were identified from the pulse-height spectrum by their gamma photo-peak energies and half-lifes. Their activities were determined from gamma photo-peak area and detection efficiencies at the photo-peak energy. The accuracy of the full-energy peak efficiency calibration for our concrete sample geometry was 5%. From the measured photo peak count rate we calculated the saturated activity (A_∞) for the most important long-lived nuclides that are found in research reactor shielding after some decades of reactor operation [1].

4. Comparison of concrete activation

Seven long-lived gamma emitting activation products (^{54}Mn, ^{60}Co, ^{65}Zn, ^{133}Ba, ^{134}Cs, ^{152}Eu and ^{154}Eu) found in activated concrete were selected for further analysis on the basis of previous studies [1]. They were selected mainly due to their important contribution to the total activity of activated concrete and due to their long decay times. Radioactive isotopes of europium, cobalt, caesium and zinc are produced in thermal and resonance neutron absorption (n,γ) reactions from trace elements present in raw materials used in concrete production. All these four trace elements can be found in almost any type of concrete ([13] and [14]). On the other hand, long-lived radioactive isotope of barium (^{133}Ba) is produced in neutron absorption (n,γ) reaction in barium, the most abundant chemical element in barite concrete. Radioactive isotope of manganese ^{54}Mn is primarily a product of fast neutron reaction (n,p) on iron isotope ^{54}Fe. Iron is also present in almost all concrete types. Measured saturated activity density for these seven isotopes in concrete samples for eight different concrete depths are presented in Fig. 5 together with calculated values for the same isotopes. The activation rates of selected nuclides presented in Fig. 5 were calculated using ORIGEN-S code [3]. The neutron fluxes used for activation calculations were taken from appropriate results of the TORT code [4]. Both codes are part of the SCALE 4.4a [15] computer program package. For the six isotopes (^{60}Co, ^{65}Zn, ^{133}Ba, ^{134}Cs, ^{152}Eu and ^{154}Eu) the experimental activation is approximately two to five times greater than calculated. The discrepancy for ^{54}Mn is something smaller.

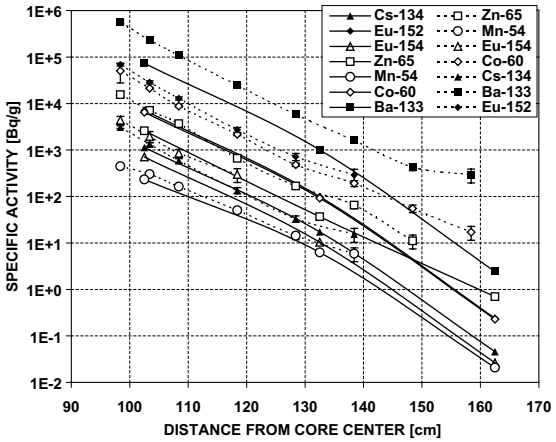

Fig. 5. Measured (dotted lines) and calculated (solid lines) saturated activity density of long-lived nuclides in barite concrete samples in different depths of the sample-holder.

Here we also mention few long-lived isotopes, which do not emit any γ rays with energies above 30 keV, but are produced by neutron irradiation of elements commonly found in natural materials. These elements have a low radiological impact due to low radiation yields [16], but should be listed for completeness. Among those are α emitting ^{232}Th and β emitters ^{3}H, ^{14}C, ^{35}Cl, ^{55}Fe and ^{151}Sm. All these isotopes cannot be detected with normal γ spectroscopy. However, we know that measured γ activation of concrete is a good indicator of neutron penetration depth. And so the activation depth profiles of mentioned α and β emitters are the same as activation depth of measured γ emitting isotopes.

5. Time evaluation of concrete activation

The time evolution of concrete activation in reactor body was calculated using ORIGEN-S code [3]. The concrete activities in different depths in the reactor body were calculated using calculated neutron flux at core mid-plane (presented in Fig. 3). This calculation was repeated for different irradiation and cooling times. Activities were calculated for different uninterrupted irradiation times from 1 to 40 years and different decay times from 1 to 100 000 years.

The calculated total specific activities of barite concrete at depth of 4.1 cm for different cooling times after reactor shut down are presented in Fig. 6 for four different irradiation times. In can be seen that for cooling times shorter than 100 years the total activity is almost the same for all irradiation times longer than 10 years.

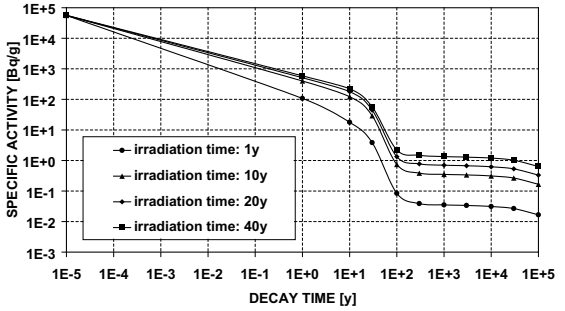

Fig. 6. Calculated time dependence of specific activity of barite concrete after shutdown at depth 4.1 cm for four different uninterrupted irradiation times.

In this irradiation period all important long-lived nuclides reach their saturated activities.

The contributions of particular isotopes to total activity are presented in Fig. 7 as the function of cooling time for the same time interval as in previous figure. Fig. 7 shows the isotopic composition of barite concrete at 4.1 cm depth irradiated for 40 years at the reactor core mid-plane. Several short-lived products, which are not presented in this figure, contribute to the total activity immediately after irradiation. After a year of cooling the total activity is dominated by the activity of ^{133}Ba at all concrete depths. Only after more than 100 years of cooling the total activity follows the decay shape of ^{41}Ca. Half-life of ^{133}Ba is 10.53 years and decays with electron capture emitting several γ rays. Half-life of ^{41}Ca, which emits no γ rays, is 103 000 years. Both isotopes are generated mostly by neutron capture reactions (n,γ) from their parent isotopes ^{132}Ba and ^{40}Ca. The natural abundance of ^{132}Ba in element barium is 0.101% and so the radioactive ^{133}Ba can be found only in activated barite concrete. On the other hand ^{40}Ca is the major natural isotope of calcium and is found in all types of concrete.

It can be concluded that ^{133}Ba and ^{41}Ca determine the quantity of activated heavy concrete for long term disposal as nuclear waste after reactor dismantling. The quantity of activated concrete that would have to be treated as nuclear waste could be estimated if clearance levels for unregulated disposal were known. However, neither the IAEA nor the EU basic standards [16,17], do not include the clearance levels for unregulated disposal for ^{133}Ba or ^{41}Ca. In our further analysis we arbitrarily selected 1 Bq/g as the 'clearance level' for both isotopes. The value was determined on the basis of values for other similar isotopes (e.g. ^{45}Ca, ^{60}Co, ^{131}Ba, ^{152}Eu) included in [16,17]. However, it should be stressed that the 'clearance levels' of 1 Bq/g for ^{133}Ba and ^{41}Ca are employed only for the purpose of this work and should be interpreted as physical parameters and not in regulatory sense. The evaluation of the clearance levels is far beyond the scope of this work.

Fig. 8 shows total activity of heavy concrete shield at different radial distances from the core centre as a function of cooling time after irradiation at full power for 40 years. These results were used for preliminary determination of activated concrete volume in shield of TRIGA Mark II research reactor at JSI. Using the limit of 1 Bq/g as the 'clearance level', the reactor body should be treated as radioactive waste to the depth of more than 1 m in the core mid-plane (see Fig. 8) immediately after reactor shut down. From the maximum depth of activated concrete in core mid-plane we can estimate its volume assuming simple and conservative spherical symmetry of activation around the core. The activated concrete volumes calculated this way are presented in Table 4. This method gives the volume of 25 m^3 immediately after reactor shutdown. After one year of cooling the total activity drops below 1 Bq/g at 74 cm, meaning 15 m^3 of activated concrete. After 10 years of cooling

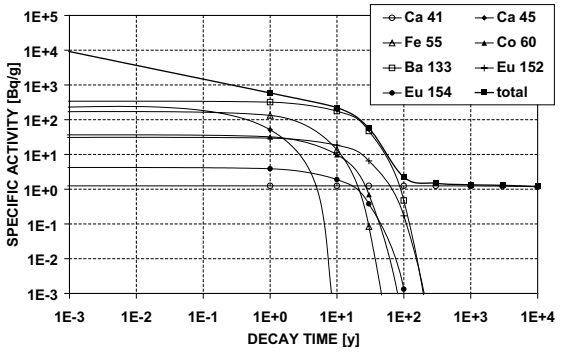

Fig. 7. Calculated isotopic specific activity versus decay time at 4.1 cm concrete depth (core mid-plane) and 40 years of irradiation time.

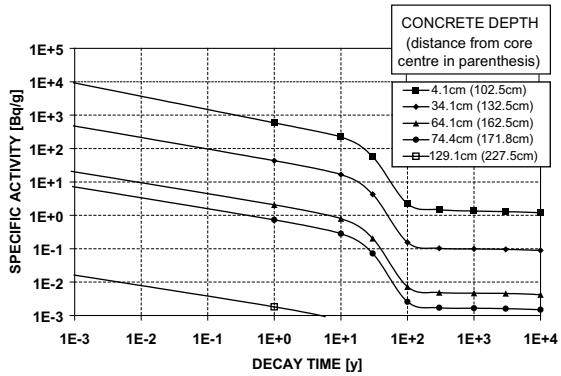

Fig. 8. Calculated total specific activity as a function of concrete depth after 40 years irradiation.

Table 4
Estimated volumes of radioactive waste from activated barite shielding of TRIGA Mark II research reactor at JSI

Cooling time (years)	Maximum activated depth (cm)	Volume (m^3)
0	100	25
1	74	15
10	64	12
100	≈5	<1

Volumes were calculated from maximum depth of activated concrete, according to the 'clearance level' 1 Bq/g.

the activity drops below 1 Bq/g in depth of 64 cm (12 m^3). And after 100 years of cooling even the activity of concrete in depth of 4 cm is less than 2 Bq/g.

6. Conclusions

Our method for determining long-term activation of the concrete based on the combination of detailed transport calculations of neutron flux inside the shield and of the experimental activation of the samples of the actual concrete yields significantly more accurate estimates on the specific activity and the volume of the activated material as the methods based on the calculations alone. The method is not sensitive to the uncertainties in the concrete composition that are main source of errors in the methods relying exclusively on calculations. The method is tested for the concrete shield of the TRIGA Mark II reactor in Ljubljana. Predominant long-lived isotope determining the volume of waste heavy concrete between 1 and 100 years of cooling is ^{133}Ba. In this time interval the waste volume halves in approximately 10 years.

Application of this method to other research reactors of similar design is straightforward. The research on the samples of TRIGA Mark II reactor in Vienna is already in progress and will be soon ready for publishing. Application of the method to the reactor shields of significantly different design (e.g. in power reactors) would require new computer modelling of the shield and spectrum adjusting in the irradiation facility by selecting appropriate inserts. The research in this direction has started for the PWR concrete shield design taking the Krško NPP as practical example.

An unexpected by-product of our research is also observation, that the clearance levels of the most important isotopes ^{133}Ba and ^{41}Ca for concrete radioactive waste disposal are not included in the international standards and regulations [16,17]. To facilitate dismantling and decommissioning process of research reactors in several countries this regulatory gap should be filled on international level as soon as possible.

References

[1] T. Žagar, M. Ravnik, Nucl. Technol. 140 (2002) 113.
[2] I. Mele, M. Ravnik, A. Trkov, Nucl. Technol. 105 (1994) 37.
[3] I.C. Gauld, O.W. Herman, R.M. Westfall, ORIGEN-S: Scale System Module to Calculate Fuel Depletion Actinide Transmutation, Fission Product Buildup and Decay, and Associated Radiation Source Terms, NUREG/CR-0200, Oak Ridge National Laboratory, 2002.
[4] W.A. Rhoades, D.B. Simpson, The TORT Three-dimensional Discrete Ordinates Neutron/Photon Transport Code (TORT Version 3), ORNL/TM-13221, Oak Ridge National Laboratory, 1997.
[5] BUGLE-96, Coupled 47 neutron, 20 gamma-ray cross section library derived from ENDF/B-VI for LWR shielding and pressure vessel dosimetry applications, DLC-185, Oak Ridge National Laboratory, 1996.
[6] M. Božič, T. Žagar, M. Ravnik, in: Proceedings of the International Conference Nuclear Energy in Central Europe 2001, Portorož, Slovenija, Nuclear Society of Slovenia, paper 108, 10–13 September 2001.
[7] R. Jeraj, T. Žagar, M. Ravnik, in: Proceedings of International Conference on the New Frontiers of Nuclear Technology PHYSOR 2002, Seoul, Korea, American Nuclear Society, paper 2A-02, 7–10 October 2002.
[8] M. Ponikvar, Internal Analysis Report, Department of Inorganic Chemistry and Technology, Jožef Stefan Institute.
[9] R. Jaćimović, Radiochemistry and Radioecology Group, Department of Environmental Sciences, Jožef Stefan Institute, Private Communication.
[10] P. Kump, XRF Group, Laboratory for Atomic Spectroscopy, Department for Low and Medium Energy Physics, Jožef Stefan Institute, Private Communications.
[11] T. Žagar, M. Ravnik, R. Jeraj, in: Proceedings of 1st World TRIGA Users Conference, Pavia, Italy, LENA University of Pavia, paper 6-3, 16–20 June 2002.
[12] T. Žagar, M. Ravnik, M. Božič, in: Proceedings of International Conference Nuclear Energy in Central Europe 2001, Portorož, Slovenija, Nuclear Society of Slovenia, paper 101, 10–13 September 2001.
[13] P.A. Lavdanskij, V.M. Nazarov, N.I. Stefanov, M.V. Frontasyeva, J. Radioanal. Nucl. Chem. 131 (1989) 261.
[14] G. Hampel, W. Bernnat, U. Klaus, in: Proceedings of 1st World TRIGA Users Conference, Pavia, Italy, LENA University of Pavia, paper 6-1, 16–20 June 2002.
[15] SCALE 4.4a (Modular Code System for Performing Criticality and Shielding Analyses for Licensing Evaluation), RSICC code package C00545/MNYCP00, March 2000.
[16] Clearance levels for radionuclides in solid materials, IAEA-TECDOC-855, Vienna, 1996.
[17] Basic safety standards for the protection of health of workers and the general public against the dangers arising from ionizing radiation, Council Directive 96/29/EURATOM, Brussels, 1996.